

Exfoliation and Characterization of Bismuth Telluride Atomic Quintuples and Quasi-Two-Dimensional Crystals

Desalegne Teweldebrhan, Vivek Goyal, and Alexander A. Balandin*

Nano-Device Laboratory, Department of Electrical Engineering and Materials Science and Engineering Program, Bourns College of Engineering, University of California—Riverside, Riverside, California 92521

ABSTRACT Bismuth telluride (Bi_2Te_3) and its alloys are the best bulk thermoelectric materials known today. In addition, stacked quasi-two-dimensional (2D) layers of Bi_2Te_3 were recently identified as promising topological insulators. In this Letter we describe a method for “graphene-inspired” exfoliation of crystalline bismuth telluride films with a thickness of a few atoms. The atomically thin films were suspended across trenches in Si/SiO_2 substrates, and subjected to detail material characterization, which included atomic force microscopy and micro-Raman spectroscopy. The presence of the *van der Waals gaps* allowed us to disassemble Bi_2Te_3 crystal into its *quintuple* building blocks—five monatomic sheets—consisting of $\text{Te}^{(1)}\text{—Bi—Te}^{(2)}\text{—Bi—Te}^{(1)}$. By altering the thickness and sequence of atomic planes, we were able to create “designer” nonstoichiometric quasi-2D crystalline films, change their composition and doping, the type of charge carriers as well as other properties. The exfoliated *quintuples* and ultrathin films have low thermal conductivity, high electrical conductivity, and enhanced thermoelectric properties. The obtained results pave the way for producing stacks of crystalline bismuth telluride quantum wells with the strong spatial confinement of charge carriers and acoustic phonons, beneficial for thermoelectric devices. The developed technology for producing free-standing quasi-2D layers of $\text{Te}^{(1)}\text{—Bi—Te}^{(2)}\text{—Bi—Te}^{(1)}$ creates an impetus for investigation of the topological insulators and their possible practical applications.

KEYWORDS Bismuth telluride, 2D crystals, atomically thin films, thermoelectrics, topological insulators, graphene-like exfoliation

Bismuth telluride (Bi_2Te_3) is a unique material with potential for a diverse range of applications. Since the discovery of its extraordinary thermoelectric properties, Bi_2Te_3 has become a vital component for thermoelectric industry.^{1–3} Bulk Bi_2Te_3 -based materials are known to have the highest thermoelectric figure of merit, $ZT \sim 1.14$ at room temperature (RT). The thermoelectric figure of merit is defined as $ZT = S^2\sigma/TK$, where $S = -\Delta V/\Delta T$ is the Seebeck coefficient (ΔV is the voltage difference corresponding to a given temperature difference ΔT), σ is the electrical conductivity, and K is the thermal conductivity, which has contributions from electrons and phonons. It is clear from the ZT definition that in order to improve thermoelectric figure of merit one should increase the thermopower $S^2\sigma$ and decrease the thermal conductivity. Different approaches have been tried in order to enhance the thermoelectric properties of Bi_2Te_3 or its alloys. These approaches included the composition change from its stoichiometry, the use of polycrystalline materials with different grain sizes, intentional introduction of structural defects, and incorporation of different dopants, e.g., Sb or Se, into Bi_2Te_3 lattice. The optimization of bulk Bi_2Te_3 led to incremental improvements, but no breakthrough enhancement in ZT was achieved.

More promising results ($ZT \sim 2.4$ for p-type material at RT) were achieved with $\text{Bi}_2\text{Te}_3/\text{Sb}_2\text{Te}_3$ superlattices produced

by the low-temperature deposition.⁴ A recent study indicated that the low-dimensional structuring of BiSbTe alloys⁵ also allows for ZT enhancement to ~ 1.5 at RT. But still higher ZT values are needed for a major practical impact. It has been shown that ZT above 3 or 4 at RT are needed in order to make thermoelectric cooling or power generation competitive with conventional methods.⁶ Such an increase in ZT would lead to a “thermoelectric revolution” and allow one for much more environmentally friendly power generation and cooling.

It follows from many theoretical predictions that a drastic improvement in ZT can be achieved in low-dimensional structures where electrons (holes) are strongly confinement in one or two dimensions.⁷ Hicks and Dresselhaus⁸ predicted that ZT can be increased in a Bi_2Te_3 quantum well by a factor of ~ 13 over the bulk value. This would require a complete carrier confinement in a quantum well with a width H on the order of ~ 1 nm and an optimized position of the Fermi level. According to Dresselhaus et al.,^{7,8} quantum confinement of charge carries in quantum wells leads to a drastic ZT improvement due to the increase in the carrier density-of-states (DOS) near the Fermi level and corresponding increase in the thermopower. The crucial condition for such mechanism is quantum confinement of carriers in quantum wells, which is only possible if materials are crystalline and essentially free of defects. The thickness of the thin film required to achieve the quantum confinement conditions has to be on the order of few atomic layers.

* Corresponding author, balandin@ee.ucr.edu or <http://ndl.ee.ucr.edu>.

Received for review: 10/27/2009

Published on Web: 03/05/2010



Note that in the superlattices commonly used in thermoelectric studies the charge carriers are only partially confined if confined at all due to the small potential barrier height and relatively low material quality. The barrier height has a pronounced effect on ZT . Broido and Reinecke⁹ have shown theoretically that $ZT = 3$ can be achieved in Bi_2Te_3 superlattices with infinite potentials when the quantum well width (i.e., thickness of the thin film) is $H \sim 3$ nm. In the structures with incomplete quantum confinement the maximum ZT decreases to ~ 2.5 and the required width becomes as small as ~ 2 nm.

Balandin and Wang¹⁰ proposed a different strategy for increasing ZT in low-dimensional structures by reducing its thermal conductivity via spatial confinement of acoustic phonons, which carry bulk of heat in thermoelectric materials. The improvement of thermoelectric properties via phonon engineering^{10,11} also can be achieved in thin films or nanowires with the thickness of just few atomic layers and high quality of interfaces. In nanostructures with rough interfaces, the thermal conductivity can be reduced due to phonon scattering on boundaries and defects.^{12–14} At the same time, defects and disorder can also lead to electron mobility degradation limiting the improvement. The phonon confinement mechanism of the thermal conductivity reduction, proposed by Balandin and Wang,¹⁰ originates from the decreased phonon group velocity of the confined acoustic phonon modes, which results in the increased scattering on point defects.^{10,11} This mechanism works even in atomic films with smooth interfaces and can be utilized without strongly degrading the electron mobility.

Thus, in order to employ the full strength of the low-dimensional confinement effects for improving thermoelectric figure of merit either via the electron band-structure and phonon engineering one needs to produce quasi-two-dimensional (2D) structures with a few-atomic layer thickness and high-quality interfaces. Conventional chemical vapor deposition, electrochemical or other means, are not capable for producing such quality structures. Molecular beam epitaxy (MBE) of low-dimensional thermoelectric materials was also much less successful than that of optoelectronic or electronic materials due to the lattice mismatch and other factors. These considerations create very strong motivations for the search of alternative approaches to fabrication of the stacks of quasi-2D crystals made of Bi_2Te_3 -based materials.

A few years ago interest in the stacked quasi-2D layers of bismuth telluride received an additional impetus from a totally different direction. It has been shown that stacks of quasi-2D layers of $\text{Te}-\text{Bi}-\text{Te}-\text{Bi}-\text{Te}$ are members of a new type of recently discovered materials referred to as *topological insulators*.^{15–16} The surface state of a quasi-2D crystal of Bi_2Te_3 is predicted to consist of a single Dirac cone. Moreover, it has been shown that the layered structures of related materials such as Bi_2Se_3 and Sb_2Te_3 are also topological insulators. The particles in topological insulators coated

with thin ferromagnetic layers have manifested exotic physics and were proposed for possible applications in the magnetic memory where write and read operations are achieved by purely electric means. All these stimulate the search for methods to produce quasi-2D crystals of bismuth telluride even further.

In our recent brief report, we have shown a possibility of cleavage from bulk Bi_2Te_3 of thin crystalline films and ribbons with the thickness of just a few atomic layers.¹⁷ In this letter, we present a complete description of the “graphene-inspired” mechanical exfoliation procedure from bulk Bi_2Te_3 , which provides individual large-area quasi-2D crystals with many interesting properties. The van der Waals gaps, present in the Bi_2Te_3 crystal structure, allowed us to disassemble the bulk crystal into its quintuple building blocks—five monoatomic sheets of $\text{Te}^{(1)}-\text{Bi}-\text{Te}^{(2)}-\text{Bi}-\text{Te}^{(1)}$, which have the thickness of ~ 1 nm. We carried out detail atomic force microscopy (AFM), scanning electron microscopy (SEM), micro-Raman spectroscopy, electrical current–voltage measurements, and thermal conductivity measurements to demonstrate the unusual properties of such quasi-2D Bi_2Te_3 crystals and to demonstrate their potential for thermoelectric applications. Considering that Bi_2Te_3 materials for the thermoelectric industry are as important as silicon (Si) and silicon oxide (SiO_2) for the electronic industry, our results may have significant practical impact. The exfoliation and characterization procedures, described in this paper in detail, can lead to a new enabling technology for producing stacks of the low-dimensional thermoelectric films with complete quantum confinement of charge carriers and acoustic phonons. The described method for producing free-standing quasi-2D layers of $\text{Te}^{(1)}-\text{Bi}-\text{Te}^{(2)}-\text{Bi}-\text{Te}^{(1)}$ creates an impetus for investigation of topological insulators and their possible practical applications.

Bi_2Te_3 has the rhombohedral crystal structure of the space group $D_{3d}^5-R(-3)m$ with five atoms in one unit cell. The lattice parameters of the hexagonal cells of Bi_2Te_3 are $a_H = 0.4384$ nm and $c_H = 3.045$ nm.¹⁴ Its atomic arrangement can be visualized in terms of the layered sandwich structure (see Figure 1). Each sandwich is built up by five monoatomic sheets, referred to as *quintuple* layers, along the c_H axis with the sequence $-\text{Te}^{(1)}-\text{Bi}-\text{Te}^{(2)}-\text{Bi}-\text{Te}^{(1)}-\text{Te}^{(1)}-\text{Bi}-\text{Te}^{(2)}-\text{Bi}-\text{Te}^{(1)}-$. Here superscripts (1) and (2) denote two different chemical states for the anions. The outmost atoms $\text{Te}^{(1)}$ are strongly bound to three planar $\text{Te}^{(1)}$ and three Bi metal atoms of the same quintuple layers and weakly bound to three $\text{Te}^{(1)}$ atoms of the next sandwich. The binding between adjacent $\text{Te}^{(1)}$ layers originates mostly from the weak van der Waals forces although other long-range Coulomb forces play a role in the bonding. The stronger bonds inside the quintuple layers are of the covalent or partially ionic nature. The presence of the van der Waals gap between the quintuples results in preferential cleavage plane between the adjacent $\text{Te}^{(1)}$ layers.

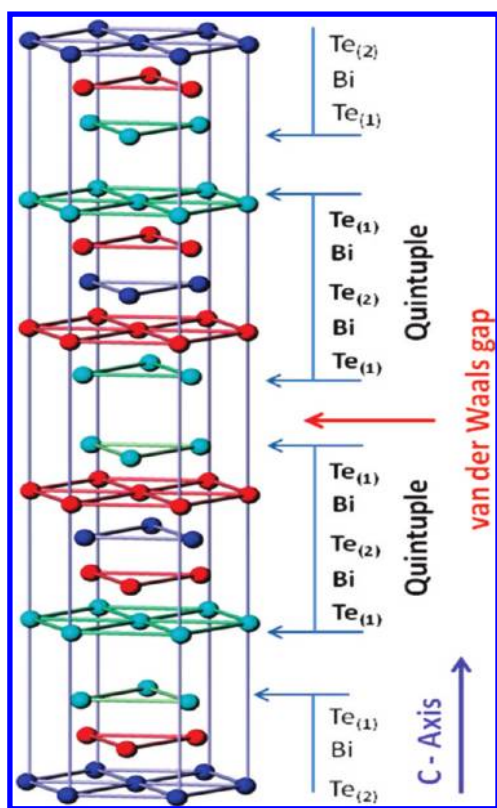


FIGURE 1. Schematic of Bi_2Te_3 crystal structure of $D_{3d}^5-R(-3)m$ space group showing quintuple layers and location of the van der Waals gaps. The $\text{Te}^{(1)}-\text{Te}^{(1)}$ bond is the weakest while the $\text{Bi}-\text{Te}^{(1)}$ bond is the strongest. The mechanical exfoliation mostly results in breaking the $\text{Te}^{(1)}-\text{Te}^{(1)}$ van der Waals bond and the formation of few-quintuples layers or quintuples.

The bond strength within the quintuple layers is not the same. The $\text{Bi}-\text{Te}^{(1)}$ bond is stronger than $\text{Bi}-\text{Te}^{(2)}$ bond, which is the second weakest point within the crystal structure. It is believed that the $\text{Bi}-\text{Te}^{(2)}$ bond is covalent while the $\text{Bi}-\text{Te}^{(1)}$ binding includes both covalent and ionic interaction. The lattice spacing between layers has a direct relationship with the atomic bond strength between the neighboring layers. For this reason the weakest $\text{Te}^{(1)}-\text{Te}^{(1)}$ bond corresponds to the largest spacing $d \sim 0.37$ nm. What is also important for our purposes is that the strength and length of the $\text{Bi}-\text{Te}^{(2)}$ bond is not much different from the van der Waals gaps of $\text{Te}^{(1)}-\text{Te}^{(1)}$. The latter suggests that the mechanical exfoliation may lead not only to $[\text{Te}^{(1)}-\text{Bi}-\text{Te}^{(2)}-\text{Bi}-\text{Te}^{(1)}]$ quintuples but also to separate atomic planes of $\text{Bi}-\text{Te}$ and $\text{Te}-\text{Bi}-\text{Te}$. One should note here that for thermoelectric applications, the quintuple layers are of greater interest than single atomic planes of Bi or Te atoms. For this reason, in this study we are mostly interested in producing individual quintuples or few-quintuple layers. The quasi-2D quintuple layers are also of principle importance for the investigation of topological insulators.

In order to isolate bismuth telluride quintuples and break them into atomic planes, we employ a method similar to the one used for exfoliation of single-layer graphene.^{18–21}

Through a mechanical cleavage process, we separated thin films from crystalline bulk Bi_2Te_3 . The process was repeated several times to obtain layers with just a few atomic planes. Owing to the specific structure of Bi_2Te_3 crystal along the c_H direction ($c_H = 3.045$ nm is a very large lattice constant as compared to other materials), we were able to verify the number of layers using the optical inspection combined with atomic force microscopy AFM, SEM, and micro-Raman spectroscopy. The thickness of the atomic quintuple is $H \sim 1$ nm. The steplike changes in the cleaved layers highest of ~ 1 nm can be distinguished well with AFM. The produced atomic layers were placed on Si substrates containing a 300 nm thick SiO_2 capping layer. The silicon oxide thickness was selected by analogy with that for graphene on Si/SiO_2 .^{18–21} We then isolated and separate individual crystal planes which exhibited high crystal quality with little to no structural defects. The mechanical cleavage of Bi_2Te_3 has led to a portion of quintuples with five atomic planes. In some cases we observed atomic planes with thickness smaller than that of the quintuple layers. The produced flakes had various shapes and sizes ranging from ~ 2 to $30 \mu\text{m}$. Some flakes had correct geometrical shapes indicative of the facets and suggesting a high degree of crystallinity. We selected large uniform $\text{Bi}-\text{Te}$ flakes with dimensions of $\sim 20-30 \mu\text{m}$ for fabrication of metal contacts for electrical characterization. For detailed material characterization, we suspended some of the $\text{Bi}-\text{Te}$ atomic films over trenches in SiO_2/Si substrates. The trenches were fabricated by reactive ion etching (RIE). They had a depth of ~ 300 nm and widths ranging from 1 to $5 \mu\text{m}$. By suspending the ultrathin atomic films over these trenches, we reduced the coupling to the substrate. The latter allowed us to achieve a better understanding of the intrinsic properties of the atomically thin layers.

The isolated $\text{Bi}-\text{Te}$ atomic layers were investigated using a high-resolution field-emission scanning electron microscope (XL-30 FEG) operated at 10–15 kV. The diffraction patterns of the crystalline structures of the layers were studied using transmission electron microscopy (TEM). The sample preparation for TEM (FEI-PHILIPS CM300) inspection was carried out through ultrasonic separation in ethanol ($\text{C}_2\text{H}_5\text{OH}$) solution. The sonication was most effective with $500 \mu\text{L}$ of $\text{C}_2\text{H}_5\text{OH}$ solution where the molar concentration of $\text{Bi}-\text{Te}$ films was held at a constant 1.41×10^{-1} mol/L throughout the solution. AFM studies were performed using a VEECO instrument with the vertical resolution down to ~ 0.1 nm. Raman spectroscopy was performed for better material identification and characterization of intrinsic properties of the resulting films. A micro-Raman spectrometer (Renishaw RM 2000) was used in a backscattering configuration excited with a visible laser light ($\lambda = 488$ nm). The spectra were collected through a $50\times$ objective and recorded with 1800 lines/mm grating providing the spectral resolution of $\sim 1 \text{ cm}^{-1}$ (software-enhanced resolution is $\sim 0.5 \text{ cm}^{-1}$). All spectra were recorded at very low power levels $P < 0.5$ mW measured with the power meter (Orion) at the sample

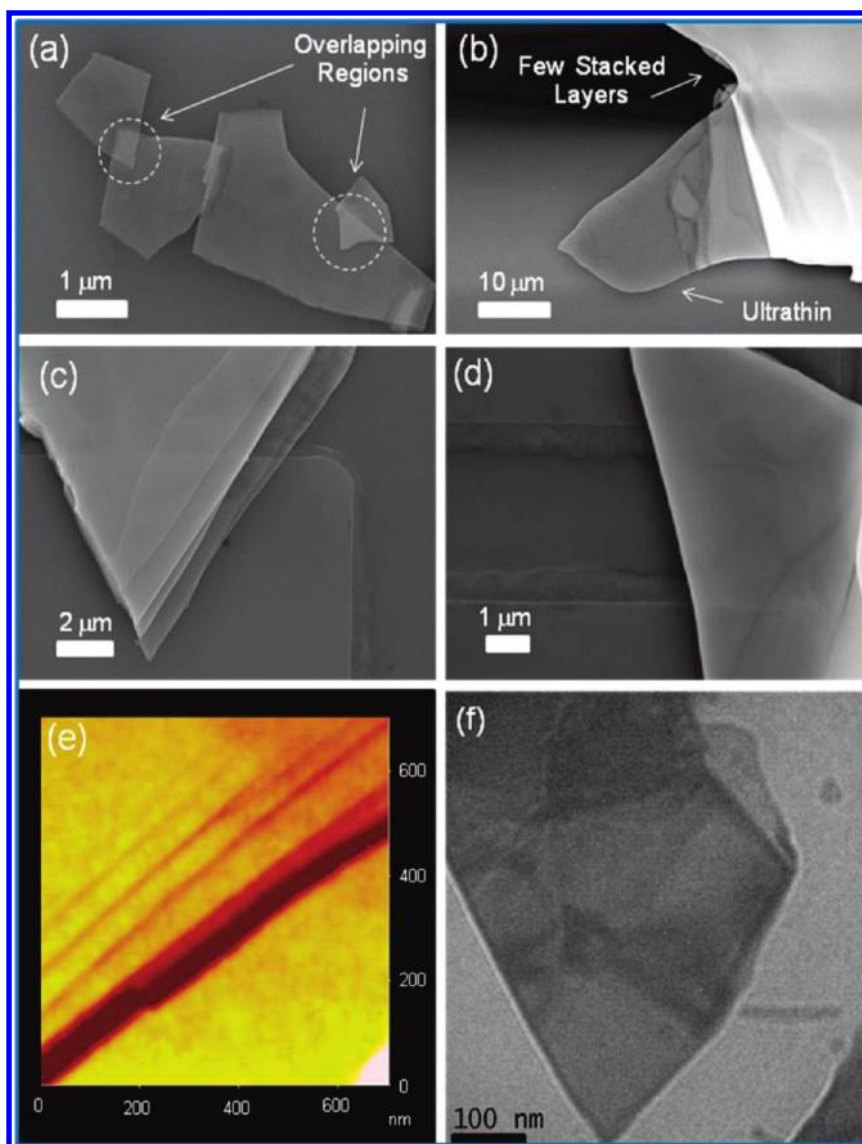


FIGURE 2. Images of quasi-2D bismuth telluride crystals showing (a) a SEM micrograph of the overlapping few-layer Bi–Te atomic crystals, (b) a large-area atomically thin crystal attached to thick Bi_2Te_3 film, (c) suspended films with visible quasi-2D layers, (d) suspended few-atom-plane film, (e) an AFM micrograph of few-atomic-layer steps in cleaved films; and (f) a TEM micrograph of quasi-2D bismuth telluride film.

surface. The low power levels were essential to avoid local laser heating, which was much more pronounced than in other material systems due to the extremely low thermal conductivity of Bi_2Te_3 . The details of our Raman instrumentation and measurement procedures were reported by us earlier in the context of graphene investigation.^{22–24} The electrodes and contact pads for the ultrathin Bi–Te layers on SiO_2 were fabricated and defined by the electron beam lithography (EBL) system (Leo 1550) followed by the metal deposition of 7 nm/70 nm Ti/Au metals with an electron beam evaporator (Temescal BJD-1800). The electrical measurements were carried out using a probe station (Signatone) at ambient conditions.

The quintuples, atomic trilayers, and bilayers were identified via combined optical, SEM, AFM, and TEM inspection. Our prior extensive experience with graphene and few-layer

graphene^{22–24} was instrumental in our ability to separate weakly distinguishable optical features in Bi–Te atomic layers placed on SiO_2/Si substrates. A relatively large thickness of the unit cell ($c_H = 3.045$ nm) made SEM and AFM identification rather effective. The representative high-resolution SEM micrographs and AFM images presented in Figure 2 show SEM, AFM, and TEM images of Bi–Te quasi-2D crystals with lateral sizes ranging from a few micrometers to tens of micrometers. In Figure 2a, one can see a SEM micrograph of high-quality crystalline films with lateral dimensions of 1–4 μm and a thickness of a few-atomic planes. Due to the atomic thickness of the films the overlapping regions are seen with a very high contrast. The larger area flakes (>20 μm) tended to be attached to thicker Bi_2Te_3 films (Figure 2b). It was our experience that for thicker films the use of the tilted SEM images was more effective in

visualizing the quintuples and atomic-layer steps. Although $[\text{Te}^{(1)}\text{--Bi--Te}^{(2)}\text{--Bi--Te}^{(1)}]$ quintuple layers were more readily available among the separated flakes, some regions of flakes had sub-1-nm thickness and appeared as protruding few-atomic-plane films. Panels c and d of Figure 2 show suspended few-quintuple films. In Figure 2e we present a typical AFM image of steps in separated films with clear layered structure. One step with a height of ~ 1 nm corresponds to a quintuple while two steps per a profile height change of ~ 1 nm indicate subquintuple units (e.g., bilayer and a trilayer). A structural analysis at nanometer scale was carried out using TEM and the selected area electron diffraction (SAED) technique. The images for this type of characterization were taken with an electron beam energy of 300 kV. The exfoliated samples were dissolved in ethanol and placed on copper grids. The TEM image in Figure 2f shows that the exfoliated Bi–Te flakes dissolved in solution retain their flat structure and do not form clusters after being subjected to ultrasonic vibrations and processing.

In Figure 3a we present an electron diffraction pattern, which indicates that the separated atomically thin layers of bismuth telluride are crystalline after all processing steps. The elemental composition and stoichiometry of the atomically thin Bi–Te layers were studied by the energy dispersive spectrometry (EDS). The data were recorded for suspended films (like those shown in panels c and d of Figure 2). Representative EDS spectra for a suspended quasi-2-D crystal and a thick Bi_2Te_3 film (used as a “bulk” reference) are shown in panels b and c of Figure 3. Note that the most pronounced peaks in Figure 3b are those of Si and oxygen (O) proving the electron beam penetration through the suspended atomically thin film. The Si and O peaks are absent in Figure 3c for thick Bi_2Te_3 crystal, which absorbs the electron beam completely.

For one of the films, which had a thickness of ~ 40 atomic planes (~ 8 quintuple layers), and occupied an intermediate position between quasi-2D crystals and bulk Bi_2Te_3 crystals, we found that the molar contents of Bi and Te were found to be $\sim 34.7\%$ and 65.3% , respectively. Although the film is crystalline and the stoichiometry for the $[\text{Te}^{(1)}\text{--Bi--Te}^{(2)}\text{--Bi--Te}^{(1)}]$ quintuple layers is preserved, one can talk about an apparent deviation from the stoichiometry due to the fact that the film is not truly bulk. For the large bulk bismuth telluride crystals used for exfoliation of the ultrathin films, we consistently found a 40–60% ratio of Bi to Te corresponding to a Bi_2Te_3 formula. The analysis of the measured EDS spectrum of the suspended film, which made up $\sim 10\%$ of the total wt %, had a molar content percentage between Bi and Te of $\sim 33.2\%$ and 66.8% , respectively. Thus, the structural make up of that particular ultrathin film has 1 to 2 ratio of Bi to Te atoms (e.g., Te–Bi–Te), which differs strongly from conventional bulk crystals.

The possibility of changing the “effective” atomic composition in the crystalline ultrathin films is very important

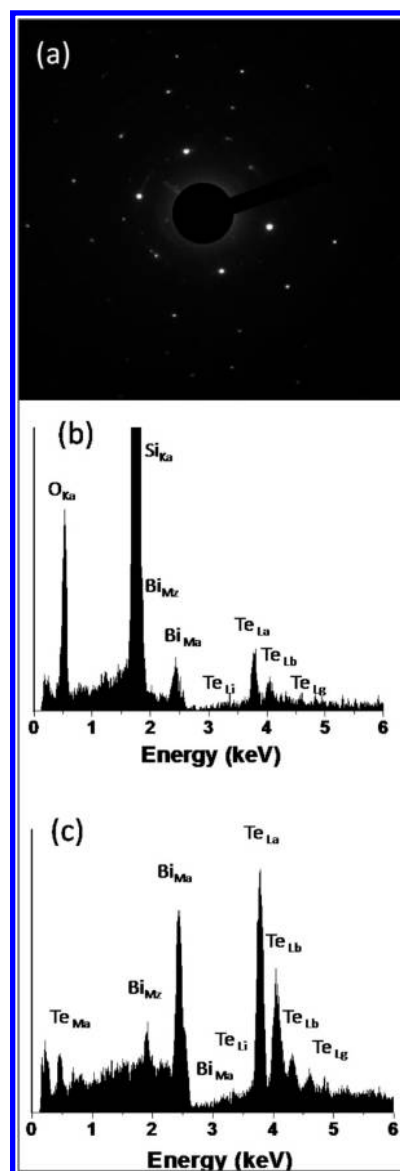


FIGURE 3. Structural and compositional characterization data showing (a) an electron diffraction pattern indicating that quasi-2D Bi–Te films are crystalline, (b) the EDS spectrum of the suspended atomic film of bismuth telluride, and (c) EDS spectrum of the reference thick film. Note that the dominant peaks in the EDS spectrum of the quasi-2D Bi–Te film shown in (b) are those of Si and O proving transparency of the atomic film for the electron beam. These peaks are absent in the spectrum of the reference bulk Bi_2Te_3 .

for practical applications. It is known from the extensive studies of the thermoelectric properties of bismuth telluride that a small variation of $\sim 0.1\%$ in the Bi to Te atomic ratio can change the properties of the material from p-type to n-type.²⁵ Intentional deviation from stoichiometry during synthesis of bismuth telluride compounds and alloys has been conventionally used for “doping” this type of material.²⁶ The close-to-stoichiometric Bi_2Te_3 is of p-type with a free carrier concentration of approximately 10^{-19} cm^{-3} . A shift to excess Te leads to an n-type material. Since our atomically thin films are crystalline, the “stoichiometric doping” may

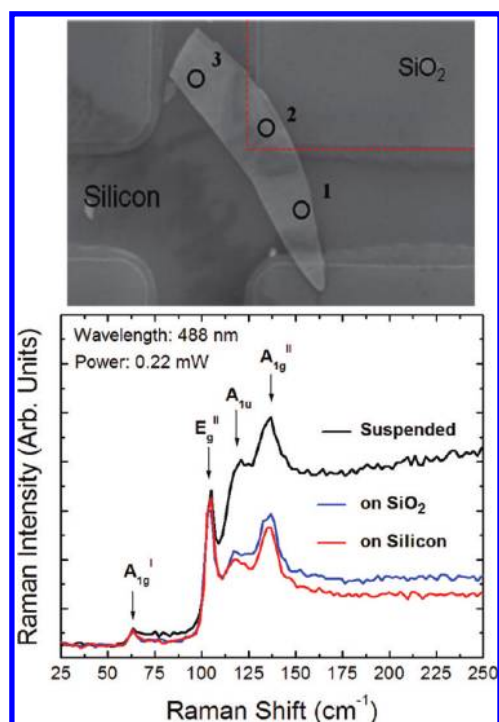


FIGURE 4. Raman spectra of quasi-2D bismuth telluride crystals. (a) SEM image showing suspended Bi–Te atomic film, which rests partially on SiO₂ and Si regions of the substrate. The spectra from the suspended and supported regions were recorded in the locations marked as 1, 2, and 3. (b) Informative Raman bands in the spectra of Bi–Te atomic films recorded at very low excitation power level. Note that the out-of-plane phonon modes in the suspended atomic crystals have higher intensity.

work in different ways than in the polycrystalline or disordered alloy bismuth telluride materials. In the atomically thin crystals, the charge can accumulate on the film surfaces or film–substrate interfaces. In this sense, the obtained quasi-2D crystals may open up a new way for doping and tuning the properties of bismuth telluride materials.

We now turn to the analysis of Raman spectrum of the atomically thin bismuth telluride films. Bi₂Te₃ has five atoms in its unit cell and, correspondingly, 15 phonon (lattice vibration) branches near the Brillouin zone (BZ) center (phonon wave vector $q = 0$).²⁷ Twelve of those 15 branches are optical phonons while the remaining three are acoustic phonons with the $A_{2u} + E_u$ symmetry. The 12 optical modes are characterized by $2A_{2u} + 2E_u + 2A_{1g} + 2E_g$ symmetry. Each of the E_g and A_{1g} modes are 2-fold degenerate. In these phonon modes, the atoms vibrate in-plane and out-of-plane (i.e., perpendicular to the film plane), respectively.²⁸ We focused our analysis on the phonon peaks in the spectral range from 25 cm⁻¹ to 250 cm⁻¹. Figure 4 shows an SEM image of the Bi–Te atomic film with locations where the Raman spectra were taken as well as the spectra themselves. These spectra were recorded at very low excitation laser power (~ 0.22 mW on the sample surface) to avoid local heating. The examined flake was placed in such a way that it had a suspended region as well as regions resting on Si

and SiO₂. The observed four Raman optical phonon peaks were identified as A_{1g} at ~ 62 cm⁻¹, E_{g2} at ~ 104 cm⁻¹, A_{1u} at ~ 120 cm⁻¹, and A_{2g} at ~ 137 cm⁻¹. These peak positions are very close to the previously measured and assigned Raman peaks of bulk crystalline Bi₂Te₃.^{27–29} Richter et al.²⁷ in their detail study of phonons in Bi₂Te₃ provided the following frequencies (in their notation): 134 cm⁻¹ for A, 103 cm⁻¹ for E_g , and 120 cm⁻¹ for A_{1u} . The A_{1u} peak is likely to become Raman active due to the symmetry breaking in atomically thin films. One can notice that the out-of-plane vibrations (at ~ 137 cm⁻¹ and ~ 119 cm⁻¹) in the suspended Bi–Te atomic films have higher intensity. The latter may be an indication of the enhancement of these vibration modes in the atomically thin films, which are not supported by the substrate. The Raman study confirms that the exfoliated films are crystalline and atomically thin. A systematic study of the changes in Raman spectrum due to modification of the vibration modes in the exfoliated ultrathin films suspended or supported on the substrate was complicated due to pronounced local heating effects.

Bulk single crystal Bi₂Te₃ is known to have very low thermal conductivity of ~ 1.5 – 2.0 W/(m K) along the cleavage plane and 0.6 W/(m K) along the van der Waals bonding direction.³⁰ It also has a low melting point of 573 °C. The local laser heating was a major problem when we tried to increase the excitation power to the levels conventionally used for other materials. The maximum excitation power of the Ar⁺ laser (with the wavelength of 488 nm) used in this study was 10 mW. Approximately half of the excitation power reaches the sample surface after transmission through the optical system. The use of the power levels above 0.5 mW (corresponding to ~ 0.22 mW on the sample) resulted in appearance of the holes due to local melting or oxidation of the atomically thin flakes as seen in the inset to Figure 5. In this image 100 % corresponds to the power of 10 mW set at the laser. We observed reproducibly that the diameter of the laser burned holes was growing with increasing excitation power (the exposure time for each spot was 100 s). Figure 5 shows an evolution in Raman spectra of Bi–Te atomic layers as the excitation power changes. When the power is too low (0.1 mW), no spectrum is excited. The excitation power of 0.5 mW provides meaningful spectra, which are in line with those obtained for bulk Bi₂Te₃ (at this power level no hole-burning or other laser-induced structural disorder was observed in microscopy images). As the power grows higher than 0.5 mW the Raman spectrum begins to change as a result of the local melting or oxidation of the material. No laser damage was observed for the bulk Bi₂Te₃ at these power levels. For this reason, the selection of the right excitation power for Raman spectroscopy of the atomically thin Bi–Te layers is crucial for obtaining informative phonon bands. The drastically different reaction of the films on laser heating confirms their few-atomic layer thickness.

The observed easy local heating damage to Bi–Te atomic flakes was in sharp contrast to graphene, a material char-

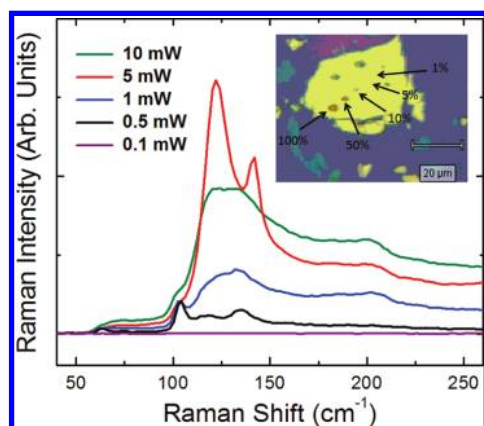


FIGURE 5. Evolution of Raman spectra from the Bi–Te atomic film with changing intensity of the excitation laser power illustrating a very narrow range of power levels suitable for exciting informative phonon bands. The power levels above 0.5 mW (corresponding to ~ 0.22 mW on the sample surface) lead to local melting of the atomic Bi–Te crystals in sharp contrast to graphene. The inset shows the spots from which the Raman spectra were recorded. Note the burned holes in the atomic films when the excitation power is above 0.5 mW.

acterized by extremely high thermal conductivity.^{31,32} We were able to use much higher laser power on suspended graphene without inflicting any damage to its lattice. The heat conduction in strictly 2D systems is a complicated subject deserving special consideration. The thermal conductivity of conventional thin films usually decreases with decreasing film thickness as a result of the acoustic phonon–boundary scattering.^{12,13} At the same time, it is also known that the thermal conductivity limited by crystal anharmonicity (also referred to as intrinsic) has a logarithmic divergence in a strictly 2D system.³³ This anomalous behavior of the 2D thermal conductivity has been studied extensively for many different crystal lattices and atomic potentials.^{34,35} One needs disorder (e.g., extrinsic scattering mechanisms) in order to obtain a finite value of the thermal conductivity in 2-D systems or limit the lateral size of the system.^{33–35} In our case of Bi–Te flakes, the samples had a thickness of several atomic layers (not exactly 2D system but rather a quasi-2D) and the extrinsic effects were dominant. Due to the very low thermal diffusivity and thermal conductivity of Bi₂Te₃ crystals at first place, the induced heat had not escaped fast enough from the local spots leading to the lattice melting and observed lattice damages. As a consequence, for thermoelectric applications, it would be better to use stacks of bismuth telluride quintuple layers, put one on top of the other, rather than atomic bilayers. Indeed, quintuples are more mechanically robust and expected to have even lower thermal conductivity than Bi₂Te₃ bulk values. In our initial report¹⁷ on the atomically-thin crystalline films of Bi₂Te₃, we were not able to present quantitative data for their thermal conductivity. Below, we report the results of the measurement of the thermal

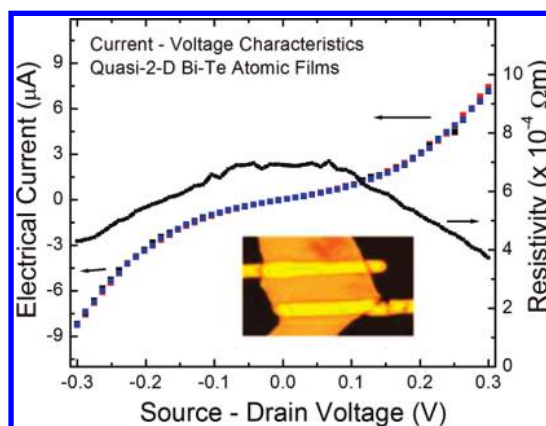


FIGURE 6. Electrical current and resistivity of the quasi-2D bismuth telluride crystal as functions of the applied source–drain bias. The inset shows an optical microscopy image of the test structure.

properties of the stacks of the mechanically exfoliated Bi₂Te₃ films.

It is also important to understand if the electrical conductivity of bismuth telluride undergoes changes after it was structured to the large-area films with the thickness of just few quintuples. For room temperature transport measurements Bi–Te devices with a bottom gate and two top metal contacts were prepared (see inset to Figure 6). The RT current–voltage characteristics shown in Figure 6 reveal a weak nonlinearity and rather low electrical resistivity on the order of 10^{-4} Ω m. This value (which includes contact resistance) is comparable to the resistivity values measured for evaporated Bi₂Te₃ films used in thermoelectric devices.^{36,37} The latter suggests that the charge carriers are not depleted in the samples and that the atomically thin bismuth telluride films retain their electrical properties. We did not observe a strong gating effect for Bi–Te devices while sweeping the back gate bias from -50 to 50 V. That was in sharp contrast to our experiments with the back-gated graphene and few-layer graphene devices.^{38,39} In the fabrication of graphene and Bi–Te devices we followed similar procedures and used the same heavily doped Si/SiO₂ wafers. One possible explanation of the weak gating in Bi–Te atomic films can be a strong doping of the flakes due to the “stoichiometric doping” discussed above. The charge accumulation at the interfaces terminated with either Bi or Te atoms can screen the electric field produced by the back gate.

The described electrically conducting bismuth telluride quasi-2D crystals can be used as quantum wells with nearly infinite potential barriers for thermoelectric applications. The charge carriers and acoustic phonons in the crystalline quintuple layers with the thickness of ~ 1 nm will be strongly confined spatially. At the same time, any practical application of thermoelectric nanostructures requires a sufficient “bulk” volume of the material for development of the temperature gradient, in the case of cooling, or voltage, in the case of power generation. An individual quantum well would not be suitable. For this reason, we envisioned a

practical method for utilization of Bi–Te quasi-2D crystals by stacking exfoliated films one on top of the other.⁴⁰ The obtained “stacked superlattices” are expected to retain the useful properties of individual atomic films such as quantum confinement of charge carriers and reduced phonon thermal conductivity. Indeed, the potential barriers for charge carriers in such crystalline films remain very high unlike in the epitaxially grown Bi₂Te₃-based superlattices with the lattice matched barriers where the band offsets are small. The thermal conductivity in the mechanically separated and stacked layers is reduced due to the acoustic phonon–rough boundary scattering or acoustic phonon spatial confinement in exactly the same way as in the individual films. We experimentally tested a possibility of ZT enhancement in layers of stacked relatively thick exfoliated films by measuring the thermal conductivity and Seebeck coefficient, and comparing them with those of the reference Bi₂Te₃ bulk crystals, which were used for the exfoliation of the films.

The thermal conductivity K of the prototype stacked exfoliated films was determined by two different methods: the laser-flash (Netzsch LFA) and the transient planar source (TPS) technique (Hot Disk). Both techniques have been “calibrated” via comparison with the values obtained with the in-house built $3-\omega$ method,^{41–43} which is considered to be a standard technique for thin films. We have previously successfully used $3-\omega$ measurements for electrically insulating thin films with the thickness down to ~ 1 nm.⁴⁴ The Seebeck coefficient of stacked films was determined using the MMR system (SB100) consisting of two pairs of thermocouples. Details of the measurements are provided in the Methods. We found significant drop in the cross-plane (in-plane) thermal conductivity from ~ 0.5 – 0.6 W/(m K) (~ 1.5 – 2.0 W/(m K)) in bulk reference to ~ 0.1 – 0.3 W/(m K) (~ 1.1 W/(m K)) in the stacked films at RT. The thermal conductivity of stacked superlattices revealed a very weak temperature dependence suggesting that the acoustic phonon transport was dominated by the boundary scattering. It is interesting to note that the measured cross-plane K value is close to the minimum thermal conductivity for Bi₂Te₃ predicted by the Cahill model,⁴⁵ which gives the low bound of ~ 0.12 W/(m K). We have not observed substantial changes in the thermal power beyond experimental uncertainty with the measured Seebeck coefficient (~ 234 μ V/K) only slightly above its bulk reference value. The latter was attributed to the fact that the Fermi level was not optimized in these films. More research is needed to gain complete control of the carrier densities in the mechanically exfoliated films. At the same time, the measured decrease of the thermal conductivity results in the estimated ZT enhancement by about 30–40% of its bulk value. Additional ZT increase in a wide temperature range can be achieved with the cross-plane electrical gating of the Bi–Te atomic films. Some of us have recently shown theoretically⁴⁶ that a combination of quantum confinement of carriers and perpendicularly applied electric field in bismuth telluride nanostructures can be effective for ZT improve-

ment. The developed an exfoliation technique can also be extended to other thermoelectric material systems.⁴⁷ This approach is particularly promising for the thermoelectric cooling applications at low temperature because the effect is even more pronounced owing to stronger suppression of the thermal conductivity.

In conclusion, using the procedures similar to those developed for graphene mechanical exfoliation, we were able to produce high-quality bismuth telluride crystals with a thickness of few atoms. Following the initial report on the possibility of exfoliation of Bi₂Te₃,¹⁷ we performed detail characterization of the suspended quasi-2D atomic crystals of bismuth telluride using SEM, TEM, EDS, AFM, SAED, micro-Raman spectroscopy and electrical and thermal measurements. We established that by altering the thickness and sequence of atomic planes one can create “designer” non-stoichiometric crystalline films and change their properties. The electrical back-gating was found to be weak, possibly due to the non-stoichiometric doping and the interface charge screening. The Raman spectra reveal differences from those of bulk crystals, which can potentially be used for nanometrology of such films. The “stacked superlattices” made of the mechanically exfoliated bismuth telluride films have shown reduced thermal conductivity and enhanced thermoelectric properties. The obtained results may lead to completely new scalable methods for producing low-dimensional thermoelectrics and atomic-layer engineering of their properties. The described technology for producing free-standing quasi-2D layers of Te–Bi–Te–Bi–Te can be used for investigation of the topological insulators and their possible practical applications.

Methods. The first technique used for K measurements is the laser-flash technique (Netzsch LFA). By timing the heat pulse propagation through our samples of known thicknesses, we applied the transient method to measure the thermal diffusivity and thermal conductivity. The experimental setup was equipped with an adjustable xenon flash lamp for heating the sample on one end while a contactless IR detector was used to measure the temperature rise at the other end. The specific instrument used for this study had a capability to measure K in the range from below 0.1 to 2000 W/(m K). We have previously “calibrated” the laser-flash measurement technique with other standard methods for measuring thermal conductivity available in our laboratory.^{41–44} Due to the geometry of the setup the measured K has to be interpreted as mostly cross-plane component of the thermal conductivity tensor. In the experiments the light pulse “shot” hit the sample and a temperature rise was measured by an InSb IR detector. The thermal conductivity is defined as $K = \alpha \rho C_p$, where α is the thermal diffusivity of the film determined in the experiment as $\alpha = 0.139Z^2/t_{1/2}$, where $t_{1/2}$ is the measured half-rise time of temperature, C_p is the heat capacity, and ρ is the mass density of the material. For the numerical analysis of the experimental data, we used several theoretical approaches, including the Parker, Cowan,

and Clark-Taylor analysis. These analysis curves were plotted with an experimental temperature time rise in order to extrapolate diffusivity and correct the result for heat loss to side-walls of a sample holder. The bismuth telluride films were prepared from the bulk Bi₂Te₃ crystals and stacked on a Corning glass substrate. The original Bi₂Te₃ crystal was used as a bulk reference. The laser-flash measurements revealed the RT thermal conductivity of the stacked films to be ~0.1–0.3 W/(m K), which is significantly lower than that of the bulk reference sample ($K = 0.5–0.6$ W/(m K) for cross-plane and $K = 1.5–2.0$ W/(m K) for in-plane). Our results for the reference bulk Bi₂Te₃ crystal and thin films are in agreement with previously reported data for bulk and Bi₂Te₃-based nanoparticles.^{30,48}

The second TPS technique (Hot Disk) provided K values, which correspond to an averaged in-plane component of the thermal conductivity. In the TPS measurements, a thin Ni heater-sensor covered with a thin electrically insulating layer was sandwiched between two stacked films under test. The samples were heated by short electrical current pulses for a few seconds. The temperature rise in response to the dissipated heat was determined from the change in the resistance of the sensor. The time dependence of the temperature rise was used to extract the thermal conductivity from the equation⁴⁹ $\Delta\tilde{T}(\tau) = P(\pi^{3/2}rK)^{-1}D(\tau)$, where τ is the parameter related to the thermal diffusivity α and the transient measurement time t_m through the expression $\tau = (t_m\alpha/r^2)^{1/2}$, r is the radius of the sensor, P is the input power for heating the sample, and $D(\tau)$ is the modified Bessel function. The RT values obtained for thermal conductivity were ~1.1 W/(m K), which also represent a significant drop compared to the bulk reference. The Seebeck coefficient was determined using MMR system (SB100) consisting of two pairs of thermocouples. One pair was formed with the junctions of copper and a reference material (constantan wire with the known Seebeck coefficient of ~36 μ V/K). The other pair was formed with the junctions of copper and the layers under test. We modified the sample stage of the system in order to be able to use it with our thin films. The computer-controlled sample stage was attached to the cold stage refrigerator and provides a preset stable temperature during the measurement. The sample chamber was kept at pressure below 10 mTorr while in operation. The measured value was about ~234 μ V/m at RT.

Acknowledgment. The authors acknowledge the support from DARPA-SRC through the FCRP Center on Functional Engineered Nano Architectonics (FENA) and Interconnect Focus Center (IFC) as well as from US AFOSR through Contract A9550-08-1-0100. Special thanks go to Mohammad Rahman and Zahid Hossain for their help with TEM and AFM measurements. The authors are indebted to other Nano-Device Laboratory (NDL) group members for assistance with the sample preparations.

REFERENCES AND NOTES

- Ioffe, A. F. *Semiconductor Thermoelements*; Nauka: Moscow, 1956 (in Russian) or Ioffe, A. F. *Semiconductor Thermoelectric and Thermoelectric Cooling*; Infosearch: London, 1957.
- Goldsmid, H. J.; Douglas, R. W. *Thermoelectric. Br. J. Appl. Phys.* **1954**, *5*, 458.
- Wright, D. A. *Nature* **1958**, *181*, 834.
- Venkatasubramanian, R.; Siivola, E.; Colpitts, T.; O'Quinn, B. *Nature* **2001**, *413*, 597–602.
- Xie, W.; et al. *J. Appl. Phys.* **2009**, *105*, 113713.
- DiSalvo, F. J. *Science* **1999**, *285*, 703.
- Dresselhaus, M. S.; et al. *Phys. Solid State* **1999**, *41*, 679.
- Hicks, L. D.; Dresselhaus, M. S. *Phys. Rev. B* **1993**, *47*, 12727.
- Broido, D. A.; Reinecke, T. L. *Appl. Phys. Lett.* **1995**, *67*, 100.
- Balandin, A.; Wang, K. L. *Phys. Rev. B* **1998**, *58*, 1544. Balandin, A.; Wang, K. L. *J. Appl. Phys.* **1998**, *84*, 6149.
- Zou, J.; Balandin, A. *J. Appl. Phys.* **2001**, *89*, 2932.
- Chen, G.; Borca-Tasciuc, T.; Yang, B.; Song, D.; Liu, W. L.; Zeng, T.; Achimov, D. A. *Therm. Sci. Eng.* **1999**, *7*, 43–51.
- Borca-Tasciuc, T.; Achimov, D.; Liu, W. L.; Chen, G.; Ren, H.-W.; Lin, C.-H.; Pei, S. S. *Microscale Thermophys. Eng.* **2001**, *5*, 225–231.
- Feutelais, Y.; Legendre, B.; Rodier, N.; Agafonov, V. *Mater. Res. Bull.* **1993**, *28*, 591–596.
- For a review see: Qi, X.-L.; Zhang, S.-C. *Phys. Today* **2010**, (January), 33–38.
- Bernevig, B. A.; Hughes, T. L.; Zhang, S.-C. *Science* **2006**, *314*, 1757.
- Teweldebhran, D.; Goyal, V.; Rhaman, M.; Balandin, A. A. *Appl. Phys. Lett.* **2010**, *96*, 053107.
- Novoselov, K. S.; Geim, A. K.; Morozov, S. V.; Jiang, D.; Zhang, Y.; Dubonos, S. V.; Grigorieva, I. V.; Firsov, A. A. *Science* **2004**, *306*, 666.
- Novoselov, K. S.; Jiang, D.; Schedin, F.; Booth, T. J.; Khotkevich, V. V.; Morozov, S. V.; Geim, A. K. *Proc. Natl. Acad. Sci. U.S.A.* **2005**, *102*, 10453.
- Novoselov, K. S.; Geim, A. K.; Morozov, S. V.; Jiang, D.; Katsnelson, M. I.; Grigorieva, I. V.; Dubonos, S. V.; Firsov, A. A. *Nature* **2005**, *438*, 197–200.
- Zhang, Y.; Tan, J. W.; Stormer, H. L.; Kim, P. *Nature* **2005**, *438*, 201–204.
- Calizo, I.; Balandin, A. A.; Bao, W.; Miao, F.; Lau, C. N. *Nano Lett.* **2007**, *7*, 2645.
- Calizo, I.; Bao, W.; Miao, F.; Lau, C. N.; Balandin, A. A. *Appl. Phys. Lett.* **2007**, 201904.
- Calizo, I.; Bejenari, I.; Rahman, M.; Liu, G.; Balandin, A. A. *J. Appl. Phys.* **2009**, *106*, No. 043509.
- Jones, P.; Hubera, T. E.; Melngailis, J.; Barryb, J.; Ervin, M. H.; Zhelevac, T. S.; Nikolaevad, A.; Leonid, Konopkod; Graf, M. *IEEE Int. Conf. Thermoelectrics* **2006**, 693.
- Golia, S.; Arora, M.; Sharma, R. K.; Rastogi, A. C. *Current Appl. Phys.* **2003**, *3*, 195–197.
- Richter, W.; Kohler, H.; Becker, C. R. *Phys. Status Solidi B* **1977**, *84*, 619.
- Russo, V.; Bailini, A.; Zamboni, M.; Passoni, M.; Conti, C.; Casari, C. S.; Li Bassi, A.; Bottani, C. E. *J. Raman Spectrosc.* **2008**, *39*, 205–210.
- Lu, W.; Ding, Y.; Chen, Y.; Wang, Z. L.; Fang, J. J. *Am. Chem. Soc.* **2005**, *127*, 10112–10116.
- Cahill; et al. *J. Appl. Phys.* **2003**, *93*, 2. Chiritescu, C.; Mortensen, C.; Cahill, D. G.; Johnson, D.; Zschack, P. *J. Appl. Phys.* **2009**, *106*, No. 073505.
- Balandin, A. A.; Ghosh, S.; Bao, W.; Calizo, I.; Teweldebhran, D.; Miao, F.; Lau, C. N.; *Nano Lett.* **2008**, *8*, 902. Ghosh, S.; Calizo, I.; Teweldebhran, D.; Pokatilov, E. P.; Nika, D. L.; Balandin, A. A.; Bao, W.; Miao, F.; Lau, C. N. *Appl. Phys. Lett.* **2008**, *92*, 151911.
- Nika, D. L.; Ghosh, S.; Pokatilov, E. P.; Balandin, A. A. *Appl. Phys. Lett.* **2009**, *94*, 203103. Nika, D. L.; Pokatilov, E. P.; Askerov, A. S.; Balandin, A. A. *Phys. Rev. B* **2009**, *79*, 155413.
- Lepri, S.; Livi, R.; Politi, A. *Phys. Rep.* **2003**, *377*, 1–80.
- Basile, G.; Bernardin, C.; Olla, S. *Phys. Rev. Lett.* **2006**, *96*, 204303.
- Dhar, A. *Phys. Rev. Lett.* **2001**, *86*, 5882.

- (36) Ji, X. H.; et al. *Mater. Lett.* **2005**, *59*, 682.
- (37) Yang, J. Y.; et al. *J. Alloys Compd.* **2000**, *312*, 326.
- (38) Shao, Q.; Liu, G.; Teweldebrhan, D.; Balandin, A. A.; Rumyantsev, S.; Shur, M.; Yan, D. *IEEE Electron Device Lett.* **2009**, *30*, 288.
- (39) Liu, G.; Stillman, W.; Rumyantsev, S.; Shao, Q.; Shur, M.; Balandin, A. A. *Appl. Phys. Lett.* **2009**, *95*, No. 033103.
- (40) Teweldebrhan, D.; Balandin, A. A. Methods for Producing Atomically-Thin Bismuth Telluride Films and Stacked Superlattices for Thermoelectric and Topological Insulator Applications, invention disclosure; University of California — Riverside, December 2009.
- (41) Shamsa, M.; Liu, W. L.; Balandin, A. A.; Casiraghi, C.; Milne, W. I.; Ferrari, A. C. *Appl. Phys. Lett.* **2006**, *89*, 161921.
- (42) (a) Ghosh, S.; Teweldebrhan, D.; Morales, J. R.; Garay, J. E.; Balandin, A. A. *J. Appl. Phys.* **2009**, *106*, 113507. (b) Ikkawi, R.; Amos, N.; Lavrenov, A.; Krichevsky, A.; Teweldebrhan, D.; Ghosh, S.; Balandin, A. A.; Litvinov, D.; Khizroev, S. J. *Nanoelectron. Optoelectron.* **2008**, *3*, 44–54.
- (43) Shamsa, M.; Ghosh, S.; Calizo, I.; Ralchenko, V.; Popovich, A.; Balandin, A. A. *J. Appl. Phys.* **2008**, *103*, No. 083538.
- (44) Balandin, A. A.; Shamsa, M.; Liu, W. L.; Casiraghi, C.; Ferrari, A. C. *Appl. Phys. Lett.* **2008**, *93*, No. 043115.
- (45) Cahill, D.; Watson, S.; Pohl, R. *Phys. Rev. B* **1992**, *46*, 6131–6140.
- (46) Bejenari, I.; Kantser, V.; Balandin, A. A. *Phys. Rev. B* **2010**, *81*, 075316. Bejenari, I.; Kantser, V. *Phys. Rev. B* **2008**, *78*, 115322.
- (47) Casian, A.; Sur, I.; Scherrer, H.; Dashevsky, Z. *Phys. Rev. B* **2000**, *61*, 15965.
- (48) Dirmyer, M. R.; Martin, J.; Nolas, G. S.; Sen, A.; Badding, J. V. *Small* **2009**, *5* (8), 933–937.
- (49) Gustafsson, S. E. *Rev. Sci. Instrum.* **1991**, *62*, 797.